Pure and Applied Geophysics

Check for updates

Spatio-Temporal Variability of Pre-monsoon Convective Events and Associated Rainfall over the State of Odisha (India) in the Recent Decade

TAPAJYOTI CHAKRABORTY,[1] SANDEEP PATTNAIK,[1] (iD) VIJAY VISHWAKARMA,[1] and HIMADRI BAISYA[2]

Abstract— The state of Odisha is situated on the eastern coast of India and is highly vulnerable to massive convective activity in the pre-monsoon season (PM), i.e., from March to May; however, there is a scarcity of studies in this context using long-term datasets. Therefore, an in-depth investigation of the variability in convective events and associated rainfall during PM over the state of Odisha has been carried out for the period 2009–2018 using the European Centre for Medium-Range Weather Forecasts (ECMWF) fifth-generation reanalysis (ERA5) datasets. The convective events (severe and moderate) identified using two sets of threshold values of three different convective indices, i.e., convective available potential energy (CAPE), the K Index, and the Total Totals Index, show an increasing trend in recent years, with South Coastal Odisha (SCO) and North Coastal Odisha (NCO) showing the highest increase. Subsequently, the spatial distribution of rainfall suggests that the maximum convective precipitation (CP) is experienced over NCO and adjacent eastern districts of North Interior Odisha (NIO). The spatial distribution of the 2 m temperature suggests that there exists a strong temperature gradient between the western and eastern portions of the state. However, the gradient weakens for the years associated with the anomalous distribution of CP. The distinct tropospheric temperature difference between the lower levels (LL) and upper levels (UL) clearly suggests that the warming (cooling) of LL is associated with high (low) CP over the region. This is further established by the coherent signature of specific humidity. The frozen hydrometeors (cloud ice and snow) are the major facilitators for the occurrence of CP over the study region. The moisture transport (MT) is associated primarily with the anomalous distribution of spatial rainfall. The years with suppressed convective activity have a distinct signature of a negative MT anomaly along with anomalous north-easterly winds (as against the typical south-westerly flow). It is also demonstrated that the anomalous MT scenario is highly modulated by the land–sea temperature contrast over the region.

Keywords: Convective events, pre-monsoon season (PM), hydrometeors, moisture transport (MT).

[1] School of Earth, Ocean and Climate Sciences, Indian Institute of Technology Bhubaneswar, Khurda, Argul, Jatni 752 050, Odisha, India. E-mail: spt@iitbbs.ac.in
[2] Regional Meteorological Centre, Guwahati 781015, Assam, India.

1. Introduction

The state of Odisha is situated on the eastern coast of India. As the whole of northern and eastern India experiences a massive increase in convective activity in the pre-monsoon season (PM, March–May) (Ray et al., 2016; Tyagi et al. 2019), Odisha also receives its share. This rise in convective activity is mainly associated with the occurrence of numerous thunderstorms, which are usually accompanied by heavy rainfall, thunder, lightning, and sometimes hail. These thunderstorms cause hundreds of casualties and massive destruction of property every year. Bharadwaj et al. (2017) showed that an average of 465 deaths occur annually due to these thunderstorm events over India. Also, most deaths occur in the north-eastern and central north-eastern states, with the greatest number of deaths recorded in the states of West Bengal, Assam, Odisha, Bihar, and Jharkhand. Towering cumulus and cumulonimbus clouds are the most important features of these events. Depending on the spatial extent of these systems (single cell or multi-cell), local instability factors can last from an hour to several hours. The instability occurs due to intense surface heating and reaches its peak severity when the continental air meets warm moist air coming from the ocean.

Several studies have investigated PM thunderstorms and other convective events over the northern Indian region. Srinivasan (1962) studied the synoptic features associated with thunderstorms over the Gangetic West Bengal and found that despite favourable conditions for initiation of convection, in the absence of the southerly wind, which is responsible for the advection of moisture, thunderstorms fail to occur over the region. Srinivasan et al. (1973)

showed that the rainfall episodes that occurred over northern India during the pre-monsoon season are associated with synoptic-scale westerly troughs that bring moisture to this region, as the westerly continental airflow brings almost no moisture. Rafiuddin et al. (2009) showed that the rainfall systems in eastern India (Odisha, West Bengal, Assam) and Bangladesh are often associated with organized bow-shaped squall line systems, resulting in heavy localized rainfall and high winds. These events are often accompanied by hail and small-scale tornadoes, causing widespread devastation over eastern India (Bhattacharya & Bhattacharya, 1983). In a study by Mahanta and Yamane (2019) investigating the climatological distribution of local severe convective storms in Assam, it was found that convective storms occur all over Assam; the highest convective activity is observed in the month of April, and the convective storms have a higher probability of occurrence in the latter part of the evening. They also showed that the seasonal pattern of these storms is in direct synchronization with the times of the year when the convective heating of the lower atmosphere is at its peak. These intense convective storms are accompanied by massive lightning activity. Using observational lightning datasets for nor'westers, Midya et al. (2021) observed that the nor'westers producing surface wind speeds above 50 km h^{-1} were usually associated with total lightning counts exceeding 30 per minute. They also showed that the total lightning count increased rapidly about 10–40 min prior to the onset of high wind on the surface. Chaudhuri (2008) showed that the most common clouds during PM over eastern India are cumulonimbus and stratocumulus clouds. In another study of thunderstorms occurring over Kolkata, Nayak and Mandal (2014) showed that wind shear between 3 and 7 km, the energy-helicity index, and the vorticity generation parameter are good predictors of precipitation associated with thunderstorms. Analysing long-term trends in thunderstorm frequency, Sen Roy and Sen Roy (2021) identified three maximum thunderstorm regions in the Indian subcontinent and also found that the frequency of thunderstorm days over eastern India and the southern part of peninsular India showed a decreasing trend in the latter half of the twentieth century, followed by a

gradually increasing trend, which corresponds to the global warming scenario.

The Severe Thunderstorm Observation and Regional Modeling (STORM) project was carried out as a multi-year observational/modeling campaign with the goal of building appropriate operational early warning systems for highly damaging severe thunderstorms over various parts of India (Das et al., 2014). The data from around 500 India Meteorological Department (IMD) manned surface observatories were used, and rainfall activity was monitored through a network of about 2000 rain gauge stations spread across the country. In one of the studies over north-eastern India conducted during this project, Chakrabarti et al. (2008) analysed 62 severe events, and they concluded that Assam Valley along the Brahmaputra river basin experiences the greatest number of these events. Tyagi and Satyanarayana (2010) noted that although a single specific index is not sufficient to forecast a convective event such as a thunderstorm, the employment of a combination of stability parameters enhances the accuracy of forecasts considerably. They also classified the better-performing convective indices in the context of pre-monsoon thunderstorm prediction over eastern India. In another study, Ray et al. (2016) showed that the frequency of thunderstorms in north-eastern India was the highest during the night, while in eastern India the frequency was highest in the evening. They also found that the sub-Himalayan West Bengal and Sikkim subdivision experienced most of the thunderstorms during the night, while in the remaining states of Odisha, Bihar, and Gangetic West Bengal, thunderstorms occurred in the evening. Under this project only, the characteristics of thunder-squalls were studied extensively over several airports (Jenamani et al., 2009; Laskar, 2009; Das et al., 2010; Suresh 2005; Mohapatra 2004). Using surrogate climate experiments, Baisya et al. (2018) showed that in a warmer climate, the vertical heat flux from stratiform clouds would increase by approximately 13%, resulting in more intense mesoscale convective events, suggesting a distinct change in the pattern of monsoon low-pressure systems over the region in a climate change scenario. In another important study addressing hyper-local forecasting of convective events over Argul (Odisha), Sisodiya et al. (2019)

showed that a proper representation of soil characteristics such as temperature and moisture are critical components for improving forecast accuracy of severe convective events over the study region.

Numerous studies have been carried out to investigate the efficiency of different stability parameters in representing environments favourable for the initiation of convection and further maturing into thunderstorms (Dhawan et al., 2008; Kunz, 2007; Ravi et al., 1999; Schultz, 1989; Tyagi et al., 2011). Convective available potential energy (CAPE) is a good indicator of the initiation of convection, and it is very useful for operational forecasting over the eastern Indian region (Roy Bhowmik et al., 2008). This index provides insight into the buoyant energy available in the atmosphere along with the moist instability (Neelin, 1997). Another useful predictor of convective initiation is the K Index (KI) (George, 1960). The KI values provide information about the moisture content in the lower atmosphere and also the vertical extent of the moist layer. The Total Totals Index (TT) is a useful empirical index that is extremely relevant in the forecasting of thunderstorms and other convective events. This index takes into account the static stability conditions (in terms of the lapse rate), as well as the moisture content in the lower atmosphere. Khole and Biswas (2007) examined the utility of the TT in forecasting thunderstorms and found that the use of a threshold value of TT along with a combination of other indices could enable accurate identification of convective events.

Although several studies have been carried out on monsoon-related convective systems, to the best of the authors' knowledge, there have been no comprehensive studies related to pre-monsoon convective systems using long-term datasets over the region. However, these pre-monsoon convective systems are responsible for many deaths and destruction over this region, and hence require proper attention. This study is an effort to fill the gap. Additionally, forecasting mesoscale convective activity is still a significant challenge for the forecasting community, particularly concerning pre-monsoon convective events and associated rainfall. Therefore, augmenting our understanding of pre-monsoon convective systems over this region is important from three perspectives: (1) to characterize its pattern over the region using long-term datasets, (2) to improve the accuracy of forecasting of these events by augmenting our understanding of the major meteorological factors, and (3) to add value for disaster preparedness and mitigation. To this end, the present study investigated the variability in pre-monsoon convective events and rainfall over Odisha state in the most recent decade. A rigorous analysis was carried out to elucidate the robust mechanisms underlying the results. The paper is arranged in four sections. Section 2 describes the datasets, the results and discussion are presented in Sect. 3, and concluding remarks are presented in Sect. 4.

2. Data

The European Centre for Medium-Range Weather Forecasts (ECMWF) fifth generation reanalysis (ERA5) data (spatial resolution ~ 25 km) for the period 2009–2018 are used for this study (Hersbach et al., 2018, 2019a, 2019b). A temporal resolution of 3 h is used for the instability indices chosen for the identification of convective events (Hersbach et al., 2018). For climatological anomaly and averaged pre-monsoon analysis, monthly mean datasets are used (Hersbach et al., 2019a, 2019b). The parameters considered from ERA5 are three different convective indices (CAPE, KI, and TT), temperature, relative and specific humidity (surface and pressure levels), total and convective precipitation, three classes of hydrometeors (cloud liquid water, cloud ice, and snow), and sea surface temperature (cds.climate.-copernicus.eu). The three convective indices used in this study for the identification of convective events are obtained directly from the ERA5. The district-scale daily rainfall data from the Odisha State Government database (rainfall.nic.in) are also used for validation purposes.

3. Results and Discussion

All the analyses are carried out over the state of Odisha for the pre-monsoon season (PM), i.e., March–May, for the study period 2009–2018 (SP). According to the IMD classification, the state of

Odisha is divided into four meteorological zones (Fig. 1): North Interior Odisha (NIO), North Coastal Odisha (NCO), South Interior Odisha (SIO), and South Coastal Odisha (SCO). Hence, the majority of analyses are carried out in the context of these four meteorological zones. The analyses regarding the spatio-temporal variation in the number of convective events, the rainfall distribution, the impact of temperature and specific humidity (SH) at both the lower

and upper levels and the hydrometeor distribution, and the effects of large-scale factors such as large-scale moisture transport and land–sea contrast, are presented in separate subsections.

3.1. Convective Events

Based on three benchmark convective indices, namely CAPE, KI, and TT, the convective events are

Figure 1
The four meteorological zones of Odisha as classified by the India Meteorological Department (IMD). The dot indicates the location of the Regional Meteorological Centre, Bhubaneswar. The zones are (i) North Interior Odisha (NIO), (ii) North Coastal Odisha (NCO), (iii) South Coastal Odisha (SCO) and iv) South Interior Odisha (SIO). (Source: http://www.imdorissa.gov.in)

classified into two categories: severe convective events (SCE) and moderate convective events (MCE). The SCEs were identified for minimum threshold values of CAPE, KI, and TT kept at 2500 J kg^{-1}, 30, and 50, respectively (George, 1960; Miller, 1972; Thompson, 2006). The MCEs were identified using a lower set of thresholds, i.e., 1500 J kg^{-1} for CAPE, 25 for KI, and 45 for TT (the details of the convective indices used in this study to identify convective events are discussed in the supplementary material S1). Each grid point (25 km resolution) with the values of CAPE, KI, and TT greater than the threshold values is considered as an individual event. As 3-hourly datasets are used to identify these convective events, a grid point having values of the convective indices higher than the threshold values for two consecutive time steps has been considered a single event. However, the events identified with this method do not correspond to actual events, and there is no time series of the accumulated number of events in the PM for both SCEs and MCEs for the SP as shown in Fig. 2. From Fig. 2, it is clear that there is a distinct increasing pattern of the accumulated PM number of events for both SCEs and MCEs. Although a decline in the number of events is observed in 2014, from 2015 onwards an increasing pattern is again noted. The zone-wise time series of the number of event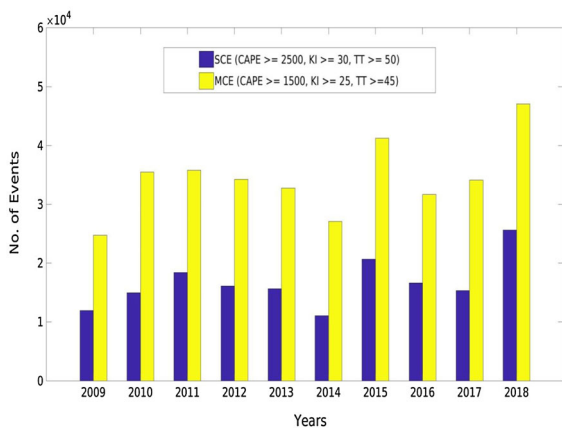s is shown in Figure S1. It is noted that all the zones show a prominent increasing trend in the number of events over the years. Figure 3 shows the spatial distribution of the accumulated PM number of events for SCEs. NCO and SCO have a more significant share of SCEs, while SIO experiences much less. NIO's eastern districts show an increasing pattern but with a moderate number (50–150 events per grid point per season) of SCEs and MCEs. An increasing pattern in the number of events (150–200 per grind point per season) is also clearly seen in Fig. 3, with 2014 being the exception (Fig. 3f). Coherent results can also be seen for the MCEs (Fig. S2).

3.2. Rainfall

Two rainfall products, total precipitation (TP) and convective precipitation (CP), from ERA5 are analysed. The spatial distribution of PM averaged TP (Fig. S3) over the years shows that the PM rainfall is usually restricted to NCO and the eastern districts of NIO, and to some extent, SCO. The TP obtained from ERA5 is also validated using the district-wise rainfall data obtained from the Odisha State Government (Fig. 4). It is seen that they are all in agreement, and both these datasets show the highest accumulated rainfall occurring in NCO, the eastern districts of NIO, and SCO, with 2014 being a year of exception (Figs. S3f and 4f). In 2014, an anomalous amount of rainfall (300–350 mm) is observed over SIO (Fig. S3f). To further segregate the type of precipitation, CP is also spatially plotted over the years (Fig. 5). It is seen that the anomalous rainfall observed in 2014 over SIO is not convective in nature (Fig. 5f). Further, the spatial extent of CP is usually restricted over NCO and the eastern districts of NIO. The eastern districts of NIO experience the greatest CP (200–300 mm), followed by NCO and SCO. It can be stated that the extent of the region experiencing CP is consistent with the region of high convective activity. To better understand the significance of MCE and SCE in terms of CP, trend and regression analyses have been carried out and are discussed in the following subsections.
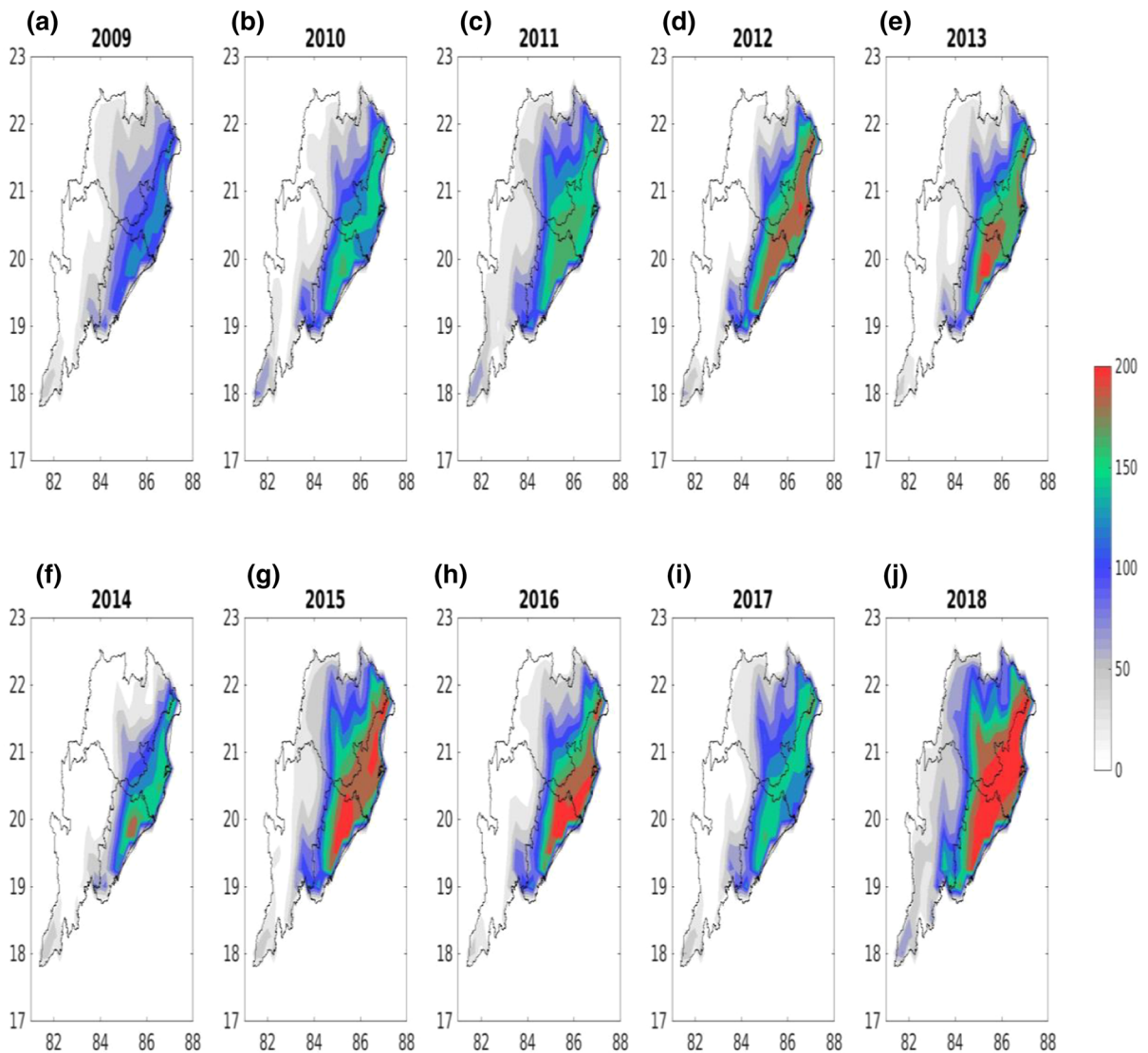

Figure 2
Time series of PM accumulated number of events for both SCEs and MCEs for the SP

Figure 3
a–j Spatial distribution of accumulated PM number of SCEs over the years in the SP

3.3. Trend Analysis

3.3.1 Regression Analysis

Regression analysis is carried out using CP data obtained from ERA5 and the number of SCEs and MCEs for all 30 districts over Odisha state for the SP. The slope of the regression equations for CP, MCE, and SCE is shown in Table 1 (columns 3, 4, and 5, respectively). Results suggest that all districts except Malkangiri (SIO) show an increasing trend in CP,

SCEs, and MCEs. This increase is smallest for the districts of SIO and is distinctly higher for NIO (eastern districts). In general, for most of these districts, MCEs show a higher increase than the SCE over the years (Table 1, columns 4 and 5, respectively). The highest increase in MCE is seen over the districts of Mayurbhanj (slope for MCE = 116.22 and slope for SCE = 73.13) and Keonjhar (slope for MCE = 103.93 and slope for SCE = 58.77), which are situated in the eastern portion of NIO. The correlation coefficients between the CP and MCE and
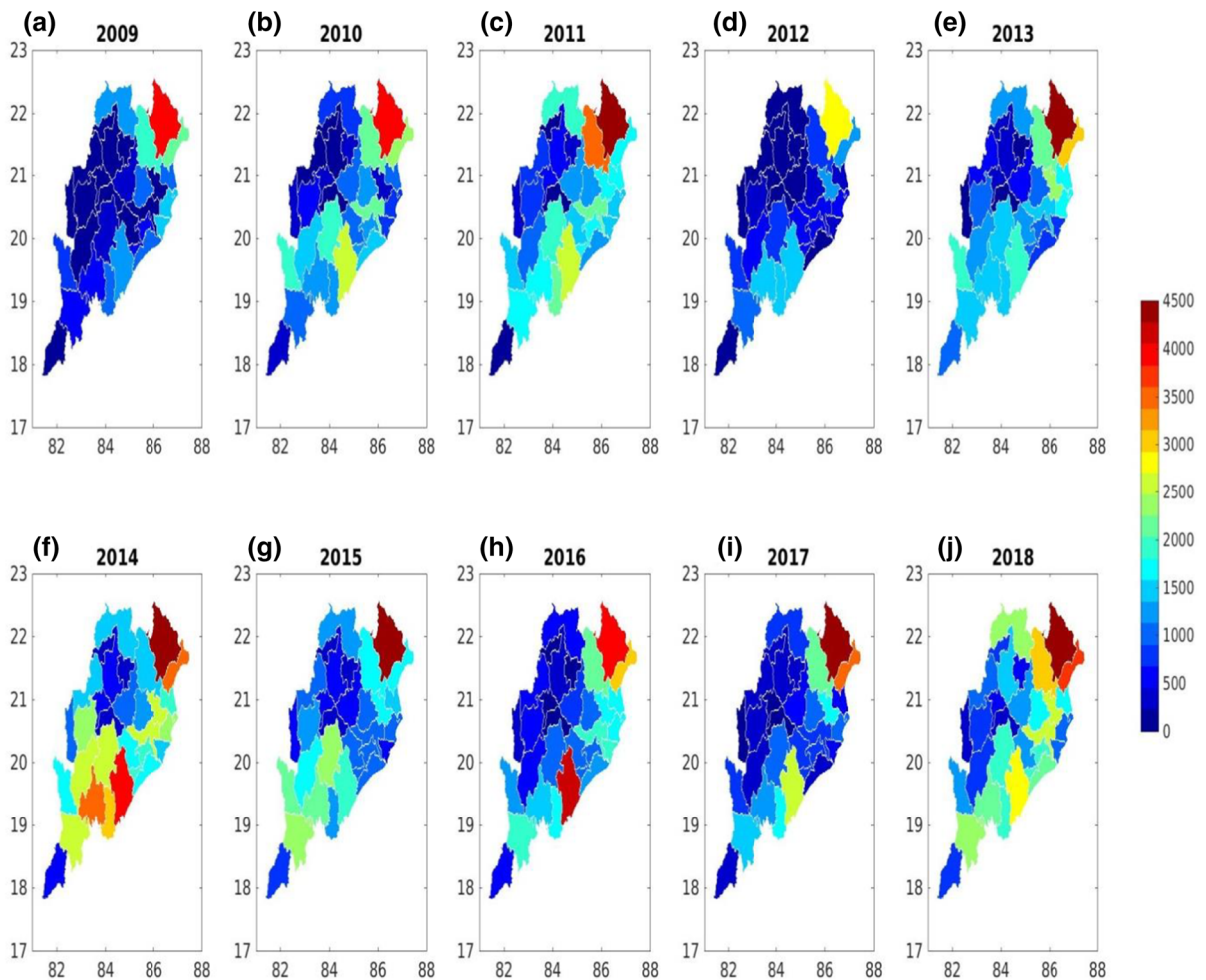
Figure 4

a–j Spatial distribution of accumulated PM rainfall (mm) over the years in the SP as per the district-wise datasets obtained from the Odisha Government Archive (rainfall.nic.in). The districts are coloured on the basis of the sum of the accumulated PM rainfall over all the stations in the district

the CP and SCE for all the districts are shown in Table 1 (columns 5 and 6, respectively). For NIO, the correlations of CP with both SCE and MCE are notably high and almost the same, indicating that these events are the major contributors to the accumulated PM CP over this meteorological zone. Furthermore, it can be seen that the correlation with the CP is higher for both MCEs and SCEs in NIO and SIO than in NCO and SCO. It can also be noted that the correlation is higher for MCEs than SCEs in most of the districts. It can be summarized that the MCEs show a greater increase than the SCEs over all the meteorological zones of Odisha, with a similar

pattern of increase in accumulated PM CP, with MCEs being the higher contributor to CP. The contribution of MCEs and SCEs to the accumulated PM CP is highest over NIO, followed by SIO.

3.3.2 Zone-wise Trend

The time series of accumulated PM number of convective events for SCEs (Fig. S4a–d), MCEs (Fig. S4e–h), and CP (Fig. S4i–m) along with their trends over the four meteorological zones of Odisha for the SP are discussed. The slopes of each of the curves are listed in Table 2. It is found that NIO has
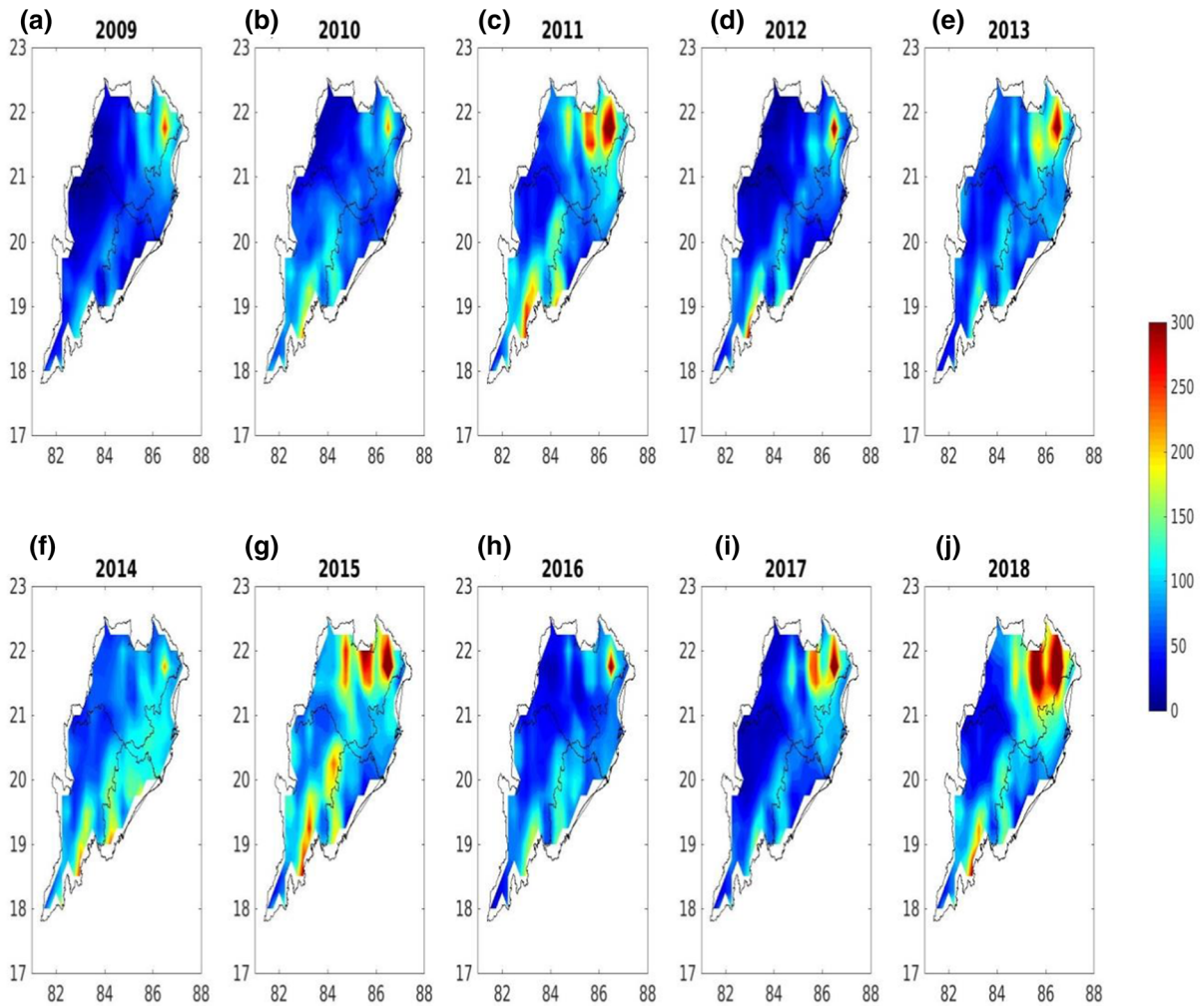
Figure 5
a–j Spatial distribution of accumulated PM CP (mm) from ERA5 data over the years in the SP

the highest slope for both SCEs (346.78) and MCEs (550.53). Although there is a considerable increasing trend in MCEs over SIO (slope = 213.9), the SCEs show the smallest increase (slope = 114.76) over SIO among the four meteorological zones. It can be noted that despite the maximum number of convective events taking place over SCO and NCO, the rate of increase for both MCEs and SCEs is highest over NIO. This scenario is further corroborated by the slope of CP over these zones, with the highest value (slope = 529.13) observed over NIO and the lowest (slope = 11.64) in SIO. The maximum increase in MCEs and SCEs is observed over NIO, and this is

corroborated by the results for the eastern districts of NIO, as seen in the regression analysis.

3.4. Temperature and Specific Humidity

The PM averaged 2 m temperature obtained from ERA5 over the state of Odisha for the SP is shown in Fig. 6. It is found that the western portion of the state is much warmer (2–3 K) than the eastern portion, and a strong temperature gradient exists from west to east. However, we see a weakening of the temperature gradient, with the temperature contrast decreasing by almost 1 K between the western and eastern portion

Table 1

The slopes for CP, MCE, and SCE for the regression analysis carried out over the years of our SP

Met. zones	Districts	Slope (CP)	Slope (MCE)	Slope (SCE)	Correlation (CP-MCE)	Correlation (CP-SCE)
NIO	Sundargarh	81.3266918	78.9272727	50.5090909	0.72717718	0.75180612
	Jharsuguda	5.36677024	8.56969697	4.04242424	0.47097173	0.33381217
	Bargarh	21.769	26.1272727	12.6242424	0.50022938	0.42518724
	Sambalpur	39.5233644	66.3939394	39.5030303	0.64092058	0.58077599
	Angul	36.7030085	72.4121212	51.5030303	0.77879757	0.73180953
	Deoghar	24.1136154	25.2242424	17.5575758	0.81517514	0.77715053
	Dhenkanal	25.6116384	52.7212121	39.1393939	0.51829862	0.46198931
	Keonjhar	129.274055	103.933333	58.769697	0.79418022	0.8457216
	Mayurbhanj	165.444956	116.218182	73.1272727	0.73443548	0.79535821
NCO	Balasore	13.4768935	28.430303	29.5575758	0.16971637	0.34230198
	Bhadrak	3.09826296	13.8666667	11.0666667	0.31301979	0.34939469
	Cuttack	27.8258462	54.7212121	42.0727273	0.40780493	0.30106897
	Jagathsinghpur	6.71141224	14.0060606	10.1393939	0.52066724	0.33447789
	Kendrapara	8.87376925	29.8181818	20.4545455	0.14866218	0.03989126
	Jajpur	19.7075983	42.5575758	30.5393939	0.28797045	0.3423527
SCO	Khurda	9.56468539	24.6909091	18.7757576	0.345472	0.15285266
	Puri	15.8730572	35.5818182	26.7939394	0.55392598	0.2914084
	Nayagarh	22.7482008	38.3878788	38.3090909	0.268461	0.31108813
	Ganjam	35.280573	62.1939394	63.5878788	0.00784372	0.10567287
	Gajapathi	5.79148039	19.969697	14.1757576	0.05955967	0.07192426
SIO	Balangir	14.7761909	24.9090909	12.7151515	0.43886006	0.23573695
	Sonepur	4.67359121	14.6363636	6.14545455	0.34071344	0.22176119
	Boudh	4.57432628	17.5090909	9.96363636	0.41044641	0.32108528
	Kandhamal	23.0965055	61.0606061	25.6	0.51746846	0.48451145
	Nuapada	11.5009538	8.11515152	4.07878788	0.41681069	0.30593858
	Kalahandi	10.7877012	28.3151515	17.7272727	0.48650874	0.37163767
	Nabrangpur	10.6591426	15.1030303	3.98787879	0.64023015	0.56290094
	Malkangiri	−3.43038036	−11.6181818	−3.60606061	0.63317886	0.65416373
	Koraput	21.3606556	13.7090909	10.1212121	0.72663659	0.64071998
	Rayagada	18.3656752	42.1636364	28.030303	0.449625	0.46540819

The correlation coefficients (obtained from the regression analysis of CP-MCE and CP-SCE) are also shown in the table

Table 2

The slopes for the trend line for CP, MCE, and SCE over the years in our SP for each meteorological zone

Parameter	NIO	NCO	SCO	SIO
CP	529.13	79.694	89.258	11.636
MCE	550.53	183.4	180.82	213.9
SCE	346.78	143.83	161.64	114.76

of the state for the years 2011, 2014, 2015, and 2018 (Fig. 6c, f, g, and j). The difference between the lower level (LL, averaged 1000–600 hPa) and upper level (UL, averaged 500–200 hPa) mean PM

temperature (shading) and SH (contours) is presented in Fig. 7. The difference in temperature between the LL and UL is higher (41–42 K) in the western portion (i.e., NIO and SIO) of the state than in the eastern portion (i.e., NCO and SCO). However, in coherence with the 2 m temperature scenario, the years 2011 (Fig. 7c), 2014 (Fig. 7f), 2015 (Fig. 7g), and 2018 (Fig. 7j) experienced a decrease in the temperature difference (39–40 K over the eastern portion vs 40–41 K in the other years, and 40–40.5 K in the western portion vs 41–42 K in the other years) between the LL and UL, indicating a weaker vertical temperature gradient and colder LL in these anomalous years. This scenario is further corroborated by the difference in specific humidity (SH) between the
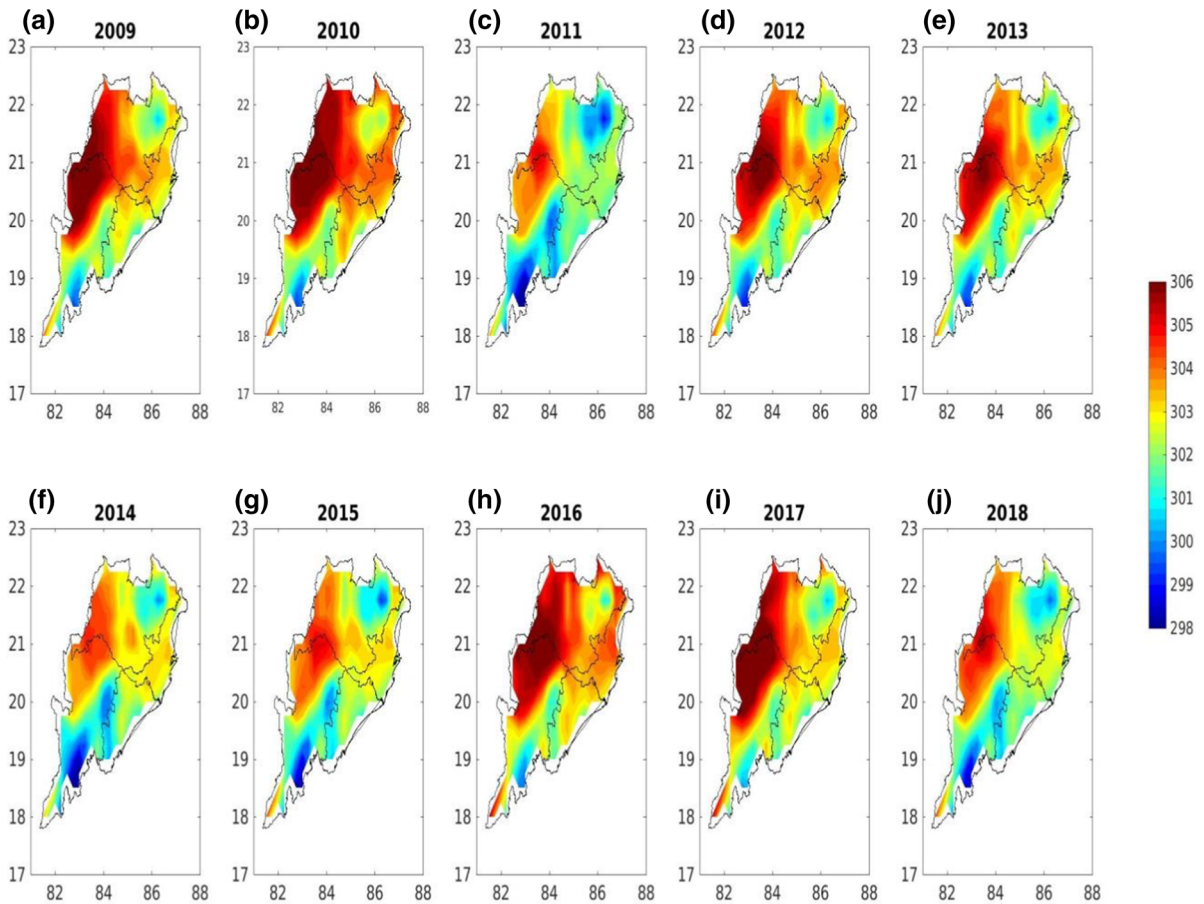
Figure 6
a–j Spatial distribution of mean PM 2 m temperature (K) over the years in the SP

LL and UL. The difference in SH between the LL and UL is higher in the eastern sector of the state than the western sector. In 2009 (Fig. 7a), 2010 (Fig. 7b), 2012 (Fig. 7d), 2013 (Fig. 7e), and 2017 (Fig. 7i), the difference is smaller. This indicates higher moisture content in the LL relative to the UL, as the spatial distribution of SH in the UL remains more or less uniform throughout the years (Fig. S5). In the remaining years, the SH difference is relatively higher, which implies comparatively lower moisture content in the LL. The years with high CP in the northern portion of the state are associated with a higher temperature contrast (40–42 K) between the LL and UL and higher moisture content in the LL, which facilitates enhanced convective activity and vertical transport of LL moisture. However, the anomalous years (i.e., 2011, 2014, and 2018) show a decrease in temperature contrast between the LL and UL and are also associated with higher SH contrast between the LL and UL, indicating lower moisture content in the LL. These results clearly indicate that LL moisture content is crucial for triggering CEs over the region, which is evidently weak during anomalous years. For further clarity, we have examined the distribution of different hydrometeors, which are discussed in the following subsection.

3.5. Hydrometeors

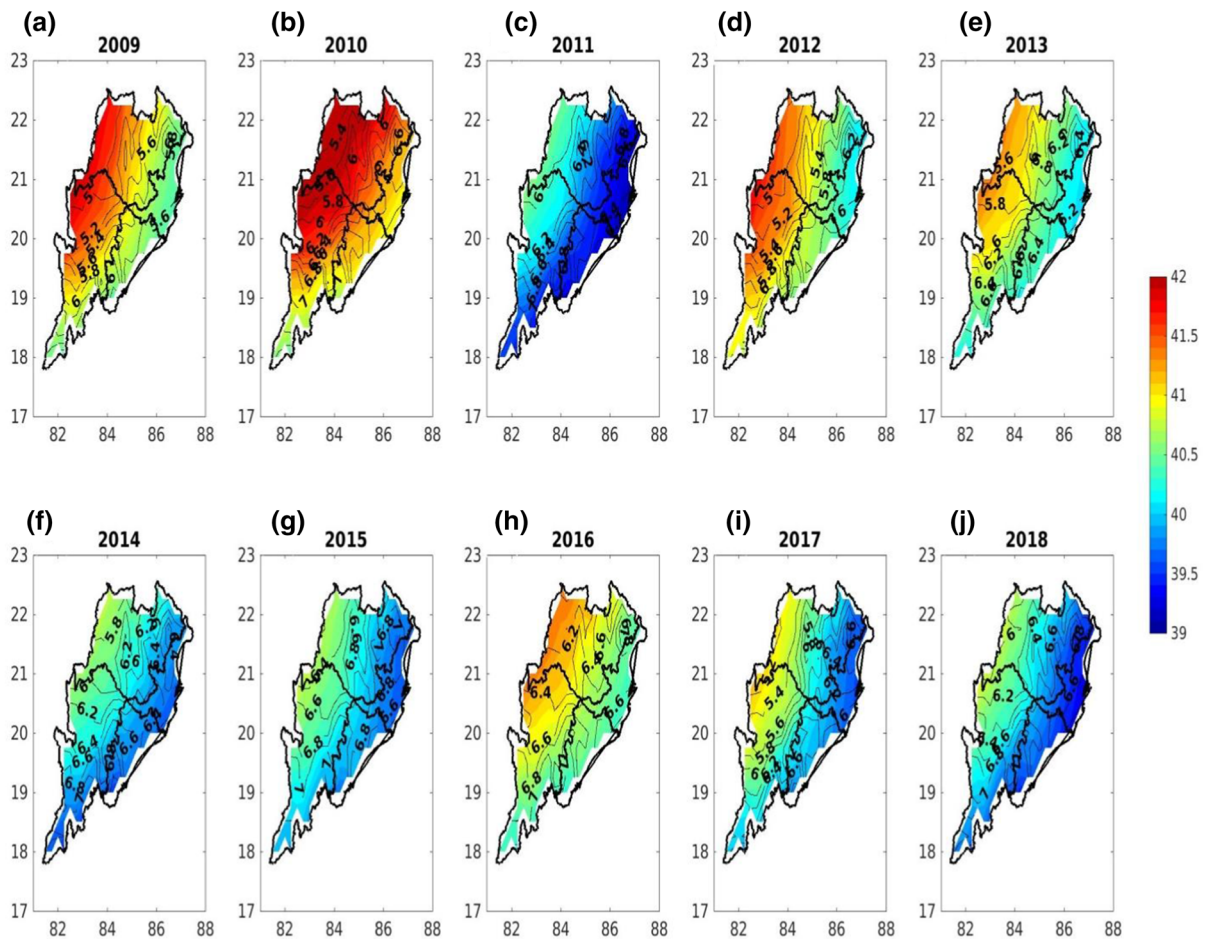To understand the variability in the microphysical scenario in the context of PM convective events,

Figure 7

a–j Spatial distributions of the difference of temperature (K, shading) and SH (kg kg^{-1}, contour) between the LL and UL over the years in the SP. The SH is scaled with the factor 10^3

three classes of hydrometeors, namely cloud liquid water (CLW), cloud ice (CI), and snow (SW), are analysed over the state of Odisha in the SP. Figure 8 shows the spatial distribution of mean CLW for the LL (1000–600 hPa) and CI for the UL (500–200 hPa). It is noted that the CLW in the LL is abundant (2.5–6 × 10^{-4} kg kg^{-1}) over NCO and SCO. However, the years 2014 (Fig. 8f), 2015 (Fig. 8g), 2016 (Fig. 8h), and to some extent 2011 show high CLW content (0.4–0.5 × 10^{-5} kg kg^{-1}) in the LL over SIO. The CI in the UL shows the highest concentration (0.6–0.8 × 10^{-5} kg kg^{-1}) over NCO and the eastern districts of NIO over the years. However, in 2011 (Fig. 8c), 2014 (Fig. 8f), and 2016

(Fig. 8h), SCO and SIO show a relatively higher concentration of CI (0.4–0.6 × 10^{-5} kg kg^{-1}) than the other years. A similar picture is seen in the case of SW (Fig. S6), with 2011 and 2012 showing less variation in SW spatially over the state of Odisha despite the highest concentration being found over NCO. The accumulation of CI and SW in the UL over the region experiencing high CP indicates the greater extent of convective clouds over the region and also the dominance of the cold-rain processes in these convective events. Further, the general distribution of CI and CLW is in agreement with the TP spatial distribution, suggesting that the mixed-phase processes are dominant in TP.
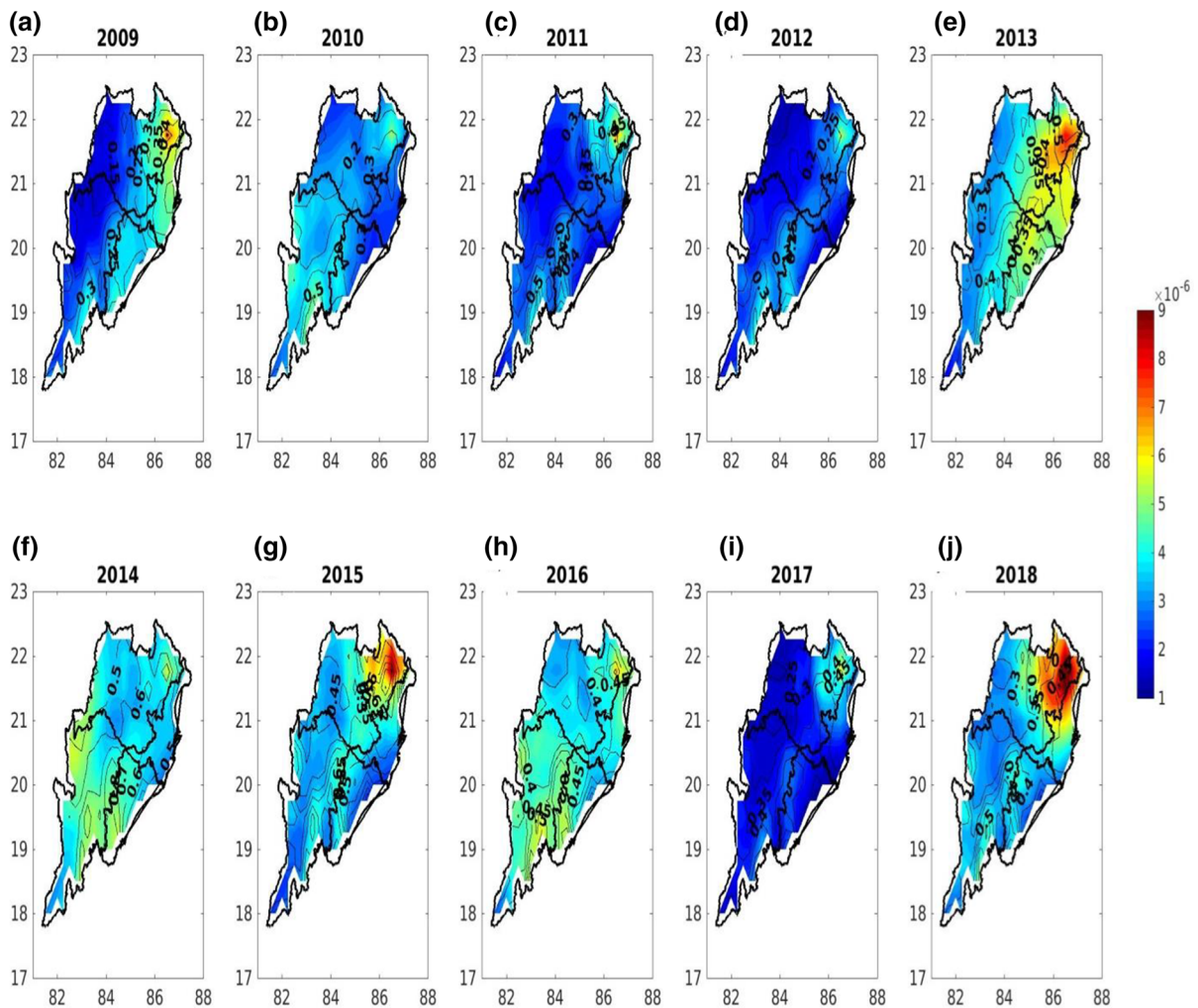
Figure 8
a–j Spatial distribution of mean PM CI in UL (kg kg^{-1}, shading) and CLW in LL (kg kg^{-1}, contour) over the years in the SP. The CLW is scaled with the factor 10^5

3.6. Moisture Transport and Land–Sea Temperature Contrast

The PM mean column integrated (1000–500 hPa) moisture transport (MT) over the Indian region is presented in Fig. S7. It is found that the mean flow over the region is south-westerly during PM. However, the climatological MT anomaly (calculated using the 30-year mean monthly data from 1989 to 2018) over the region (Fig. 9) for the SP shows an interesting aspect. The area of interest, including Odisha with the neighboring land region and the adjacent Bay of Bengal (BoB), is shown using a box bounded by 17°–23° N and 80°–90° E in both these figures. It can be seen that for the years 2010 (Fig. 9b), 2013 (Fig. 9e), and 2016 (Fig. 9h), and to some extent 2017 (Fig. 9i) and 2018 (Fig. 9j), the coastal region of Odisha and the adjacent BoB region experienced a positive MT anomaly (2–6 kg m kg^{-1}.s^{-1}). On the other hand, for 2009 (Fig. 9a), 2011 (Fig. 9c), 2014 (Fig. 9f), and 2015 (Fig. 9g), there is a high negative MT anomaly (-2 to -6 kg m kg^{-1} s^{-1}), along with anomalous north-easterly winds. It is clear that there is a periodic
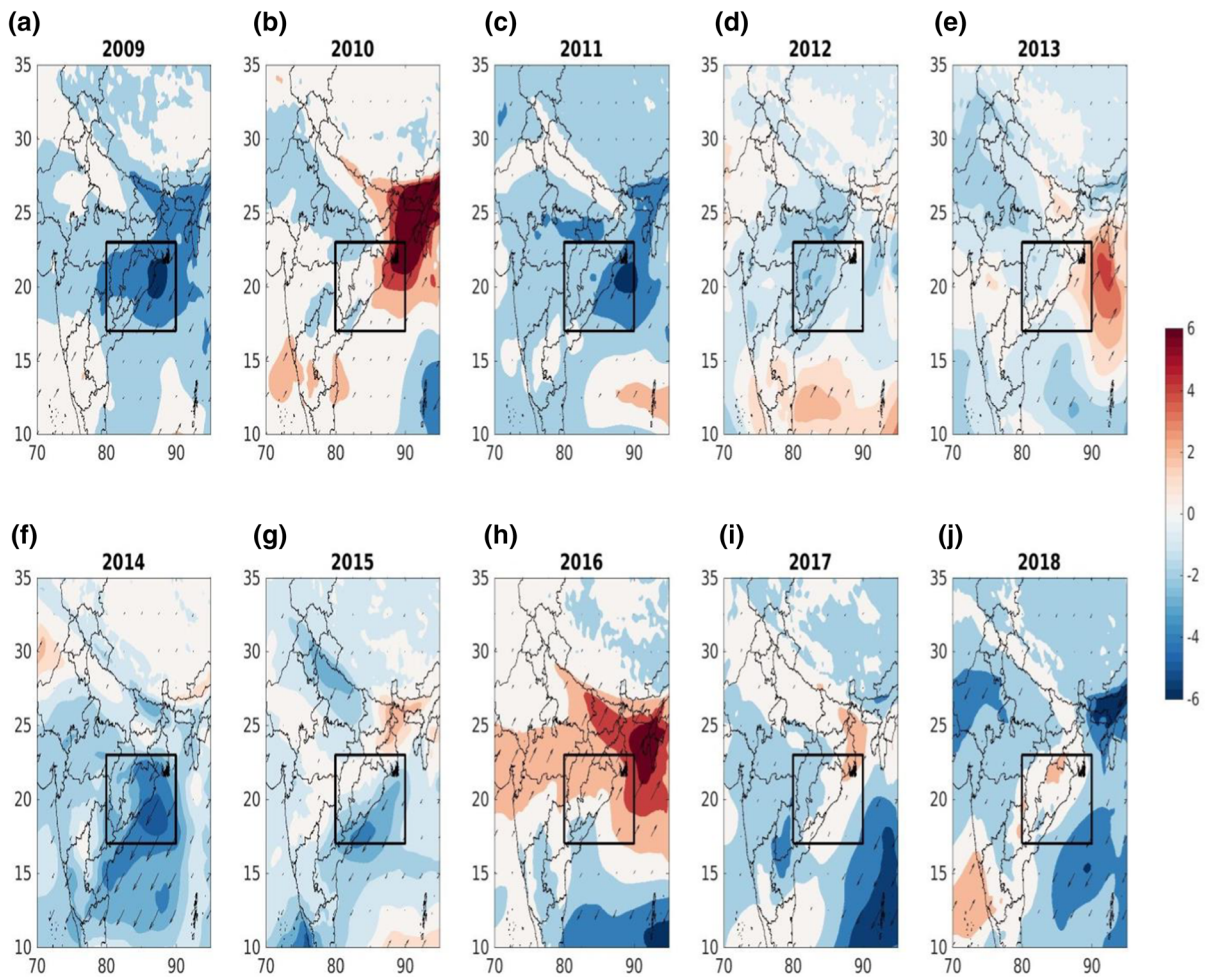
Figure 9
a–j Climatological anomaly of PM column integrated (1000–500 hPa) MT (kg m kg^{-1}.s^{-1}, shading) along with anomalous wind (vectors) over the Indian region in the SP. The box depicts the region bounded by 17°–23° N and 80°–90° E

fluctuation of the MT anomaly over the years. The MT anomaly at the surface (1000 hPa) is also shown in Fig. S8, along with the wind anomaly. It can be inferred that the surface scenario contributes significantly to the fluctuations in the column-integrated MT anomaly and the north-easterly flow dominant in the anomalous years. The negative MT anomaly over coastal Odisha and the adjacent BoB is associated with an anomalous north-easterly flow, which allows the relatively drier air to flow (reducing moisture content) over Odisha, suppressing convective activity in anomalous years.

To further identify the mechanisms driving the periodic pattern of anomalous MT, the difference between the 2 m temperature over the land and the sea surface temperature (SST) of the adjacent BoB over the region bounded by 17°–23° N and 80°–90° E (the box shown in Fig. 9) is shown in Fig. 10. It can be seen that the land–sea temperature contrast (LSTC) shows a periodic variation for the SP, which is consistent with the pattern of the MT anomaly: the LSTC attaining three maxima with approximate values of 2.7, 2.4, and 2.95 K in 2010, 2013, and 2017, respectively, and two minima with values of 1.4 and 1.5 K in 2011 and 2014, respectively. Interestingly, 2011 and 2014 are years that showed excessive negative anomalies of MT and subsequently led to anomalous spatial distribution of
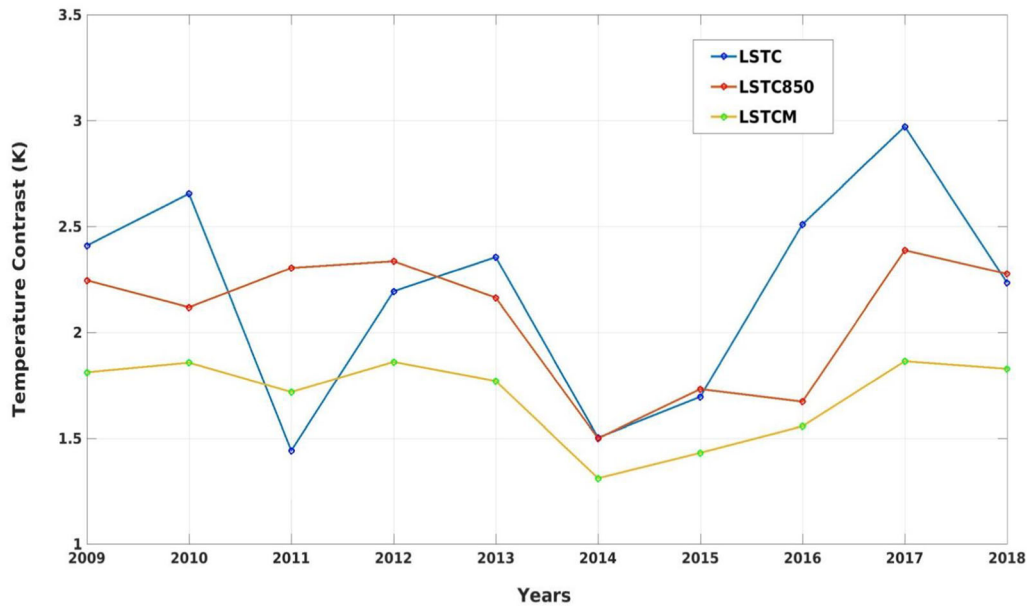
Figure 10
Time series of LSTC, LSTC850, and LSTCM (calculated over the region bounded by 17°–23° N and 80°–90° E) in K for the SP

convective precipitation. On the other hand, the years in which the maxima of the LSTC were achieved were associated with a positive MT anomaly. Along with the LSTC, the temperature contrast between the land and the sea at the 850 hPa level (LSTC850) and the contrast in mean temperature from 1000 to 500 hPa between the land and the sea (LSTCM) are shown in Fig. 10. Fluctuations can be seen for LSTC850 and LSTCM over the years, but the magnitude of the variation is less than that of the LSTC, indicating that the surface conditions have the greatest impact in the MT scenario. These results suggest that the LSTC plays a key role in modulating the MT over the region and in strongly modulating PM convective events and the rainfall associated with them. It can be inferred that in the anomalous years, the decreased LSTC influences the MT by weakening the south-westerly flow and allows an anomalous north-easterly flow to intrude and result in a negative MT anomaly over the adjacent BoB region. This leads to the weakening of convective activity over northern Odisha.

4. Conclusions

The variability in convective events and associated rainfall during PM over the coastal state of Odisha for the SP is investigated in this study. The findings of this study can be summarized as follows:

- The number of convective events (both SCE and MCE), identified using threshold values of three different stability indices (i.e., CAPE, KI, and TT), shows an increasing trend for the SP. The maximum increase in these convective events is witnessed in NIO.
- The spatial distribution of rainfall suggests that NCO and the eastern districts of NIO, followed by SCO, experience the maximum convective rainfall. However, the years 2011 and 2014 showed a prominent anomalous pattern, with SIO experiencing most of the rainfall.
- Regression analysis, employed to examine the variation in SCEs and MCEs, along with the CP at district-scale, showed that throughout the state, there is an increase in MCEs compared to the SCEs, and the eastern districts in NIO show the greatest increase in CP, SCEs, and NCEs. The

zone-wise trend analysis of CP, SCE, and MCE shows the highest increase over NIO. It should be noted that although the MCE and SCE show a considerable slope for SIO, the slope of CP was the lowest for SIO, implying that the CP experienced by SIO corresponds not only to the SCEs and MCEs occurring over the zone, but also to the residual rainfall from the stratiform rain systems. Although the maximum number of SCEs and MCEs are found over NCO and SCO, the rate of increase of these events and the corresponding CP over the SP is highest in NIO. This can be attributed to the massive increase in convective activity over the districts of Mayurbhanj and Keonjhar in the eastern NIO.

- The mean PM surface temperature shows a strong gradient from the western portion of the state (i.e., NIO and SIO) to the eastern portion (i.e., NCO and SCO), but this gradient was noted to be weaker, with temperature contrast decreasing by almost 1 K between the western and eastern portions of the state in the anomalous years (2011, 2014, 2015, and to some extent, 2018), indicating lower surface temperature over the region, which is not favourable for localized convection. In addition, the temperature difference between the LL and UL indicates that the anomalous years are associated with a weaker vertical temperature gradient and colder UL, which restricts the growth of convective clouds and thus weakens the convective activity. Furthermore, the anomalous years are associated with lower moisture abundance in LL, contrary to the moister LL seen in the other years, which further impedes strong convective activity.

- The spatial distribution of three different classes of hydrometeors is in agreement with the locations of the PM rainfall observed in the SP, indicating the influence of microphysical processes in the PM rainfall in this region. Accumulation of CI in the UL over northern NCO and the eastern NIO corroborates the high vertical extent of convective clouds and implies that the high CP experienced in this region is strongly modulated by cold-rain processes.

- From the MT perspective, the mean flow over the region is south-westerly. However, the anomalous rainfall years (i.e., 2011, 2014, and 2015) are associated with a negative MT anomaly over coastal Odisha and the adjacent BoB, along with an anomalous north-easterly flow. This scenario is further corroborated by the analysis of the temperature contrast between the land region over the state of Odisha and surrounding states and the adjacent BoB (region bounded by 17°–23° N and 80°–90° E). There is a prominent periodic pattern, with values ranging from 1.4 to 2.95 K in the LSTC over the years, which plays an important role in this scenario. It can be inferred that in the anomalous years, the decreased LSTC influences the MT by weakening the south-westerly flow, and allows an anomalous north-easterly flow to intrude and result in the negative MT anomaly over the adjacent BoB region, resulting in the weakening of convective activity over northern Odisha.

This study provides insight into the convective environment during PM over the state of Odisha and also identifies the factors modulating the convective activity. In conclusion, it can be stated that the periodic fluctuations in LSTC result in large-scale fluctuations in MT over the region, which in turn modulate the convective activity in the area. This study also distinctly demonstrates that there is an increasing trend in PM convective activity and associated CP over the region, with the highest increase seen in the eastern districts of NIO. These findings will be immensely helpful to operational forecasters, policymakers, and disaster management authorities for proactive efforts towards better preparedness and formulating a plan of action to minimize possible damage caused by these convective storms occurring in the PM at the district scale.

State Government for providing the district-wise rainfall datasets. The plots shown in this study are made with MATLAB 2017b (www.mathworks.com), and the algorithms are available on request to the corresponding author.

Publisher's Note Springer Nature remains neutral with regard to jurisdictional claims in published maps and institutional affiliations.

REFERENCES

Baisya, H., Pattnaik, S., Hazra, V., Sisodiya, A., & Rai, D. (2018). Ramifications of atmospheric humidity on monsoon depressions over the indian subcontinent. *Nature Scientific Report, 8*, 9927. https://doi.org/10.1038/s41598-018-28365-2

Bharadwaj, P., Singh, O., & Kumar, D. (2017). Spatial and temporal variations in thunderstorm casualties over India. *Singapore Journal of Tropical Geography, 38*(3), 293–312.

Bhattacharya, A. B., & Bhattacharya, R. (1983). Radar observations of tornadoes and the field intensity of atmospherics. *Meteorology and Atmospheric Physics, 32*(1–2), 173–179.

Chakrabarti, D., Biswas, H. R., Das, G. K., & Kore, P. A. (2008). Observational aspects and analysis of events of severe thunderstorms during April and May 2006 for Assam and adjoining states—a case study on 'Pilot STORM project.' *Mausam, 59*(4), 461–478.

Chaudhuri, S. (2008). Preferred type of cloud in the genesis of severe thunderstorms—a soft computing approach. *Atmospheric Research, 88*(2), 149–156.

Das, S., Mohanty, U. C., Tyagi, A., Sikka, D. R., Joseph, P. V., Rathore, L. S., Habib, A., Baidya, S. K., Sonam, K., & Sarkar, A. (2014). The SAARC STORM: a coordinated field experiment on severe thunderstorm observations and regiobal modeling over the South Asian Region. *Bulletin of American Meteorological Society, 95*(4), 603–617. https://doi.org/10.1175/BAMS-D-12-00237.1

Das, K., Samui, R. P., Kore, P. A., Siddique, L. A., Biswas, H. R., & Barman, B. (2010). Climatological and synoptic aspect of hailstorm and squall over Guwahati Airport during pre-monsoon season. *Mausam, 61*(3), 383–390.

Dhawan, V. B., Tyagi, A., & Bansal, M. C. (2008). Forecasting of thunderstorms in pre-monsoon season over Northwest India. *Mausam, 59*(4), 107–111.

George, J. J. (1960). *Weather forecasting for aeronautics*. Academic Press.

Hersbach, H., Bell, B., Berrisford, P., Biavati, G., Horányi, A., Muñoz Sabater, J., Nicolas, J., Peubey, C., Radu, R., Rozum, I., Schepers, D., Simmons, A., Soci, C., Dee, D., & Thépaut, J-N. (2018). ERA5 hourly data on single levels from 1979 to present. Copernicus Climate Change Service (C3S) Climate Data Store (CDS).

Hersbach, H., Bell, B., Berrisford, P., Biavati, G., Horányi, A., Muñoz Sabater, J., Nicolas, J., Peubey, C., Radu, R., Rozum, I., Schepers, D., Simmons, A., Soci, C., Dee, D., & Thépaut, J-N. (2019). ERA5 monthly averaged data on single levels from 1979

to present. Copernicus Climate Change Service (C3S) Climate Data Store (CDS).

Hersbach, H., Bell, B., Berrisford, P., Biavati, G., Horányi, A., Muñoz Sabater, J., Nicolas, J., Peubey, C., Radu, R., Rozum, I., Schepers, D., Simmons, A., Soci, C., Dee, D., & Thépaut, J-N. (2019) ERA5 monthly averaged data on pressure levels from 1979 to present. Copernicus Climate Change Service (C3S) Climate Data Store (CDS).

Jenamani, R. K., Vashisth, R. C., & Bhan, S. C. (2009). Characteristics of thunderstorms and squalls over Indira Gandhi International (IGI) Airport, New Delhi - impact on environment especially on summer's day temperatures and use in forecasting. *Mausam, 60*(4), 461–474.

Khole, M., & Biswas, H. R. (2007). Role of total-totals stability index in forecasting of thunderstorm/non-thunderstorm days over kolkata during pre-monsoon season. *Mausam, 58*(3), 369–374.

Kunz, M. (2007). The skill of convective parameters and indices to predict isolated and severe thunderstorms. *Nat. Haz. Earth Syst. Sci., 7*, 327–342.

Laskar, S. I. (2009). Some climatological features of thunderstorms and squalls over Patna airport. *Mausam, 60*(4), 533–537.

Mahanta, R., & Yamane, Y. (2019). Climatology of local severe convective storms in Assam, India. *International Journal of Climatology, 40*(2), 957–978. https://doi.org/10.1002/joc.6250

Midya, S. K., Pal, S., Dutta, R., Gole, P. K., Chattopadhyay, G., Karmakar, S., Saha, U., & Hazra, S. (2020). A preliminary study on pre-monsoon summer thunderstorms using ground-based total lightning data over Gangetic West Bengal. *Indian Journal of Physics, 95*, 1–9. https://doi.org/10.1007/s12648-020-01681-y

Miller, R.C. (1972). Notes on Analysis and Severe Storm Forecasting Procedures of the Air Force Global Weather Control (AFGWC). *Tech. Rep. 200 (Rev) Air Weather Services, U.S. Air Force.*

Mohapatra, M., Koppar, A. L., & Thulasi Das, A. (2004). Some climatological aspects of thunderstorm activity over Bangalore City. *Mausam, 55*(1), 184–189.

Nayak, H. P., & Mandal, M. (2014). Analysis of stability parameters in relation to precipitation associated with pre-monsoon thunderstorms over Kolkata India. *Journal of Earth System Science, 123*(4), 689–703.

Neelin, J. D. (1997). Implications of Convective Quasi-equilibria for the Large-scale Flow. In R. K. Smith (Ed.), *Physics and parameterization of moist atmospheric convection* (pp. 413–446). Kluwer Academic Publishers.

Rafiuddin, M., Uyeda, H., & Islam, Md.N. (2009). Simulation of Characteristics of Precipitation Systems Developed in Bangladesh during Pre-monsoon and Monsoon. *2nd Int. Con. Water Flood Man. (ICWFM-2009)*, 61–67.

Ravi, N., Mohanty, U. C., Madan, O. P., & Paliwal, R. K. (1999). Forecasting of thunderstorms in the pre-monsoon season at Delhi. *Meteorological Applications, 6*, 29–38. https://doi.org/10.1002/met.19996103

Ray, K., Sen, B., Sharma, P. (2016). Monitoring Convective Activity over India During Pre-Monsoon Season-2013 under the SAARC STORM Project. *Vayu Mandal., 42*(2), 106–128. http://imetsociety.org/wp-content/pdf/vayumandal/2016422/2016422_5.pdf

Roy Bhowmik, S. K., Sen Roy, S., & Kundu, P. K. (2008). Analysis of large scale conditions associated with convection over the indian monsoon region. *International Journal of Climatology, 28*, 797–821. https://doi.org/10.1002/joc.1567

Schultz, P. (1989). Relationships of several stability indices to convective weather events in Northeast Colorado. *Weather and Forecasting, 4*, 73–80. https://doi.org/10.1175/1520-0434(1989)004%3c0073:ROSSIT%3e2.0.CO;2

Sen Roy, S., & Sen Roy, S. (2021). Spatial patterns of long-term trends in thunderstorms in India. *Natural Hazards, 107*, 1527–1540. https://doi.org/10.1007/s11069-021-04644-6

Sisodiya, A., Pattnaik, S., Baisya, H., Bhat, G. S., & Turner, A. G. (2019). Simulation of location-specific severe thunderstorm events using high resolution land data assimilation. *Dynamics of Atmosphere and Oceans, 87*, 101098. https://doi.org/10.1016/j.dynatmoce.2019.101098

Srinivasan, V., Ramamurthy, K., & Nene, Y.R. (1973). Discussion of Typical Synoptic Weather Situation, Summer Nor'westers and Andhis and Large Scale Convective Activity over Peninsula and Central Parts of the Country. *F.M.U. Rep*., No. III-2.2, India Meteorological Department.

Suresh, R., & Bhatnagar, A. K. (2005). Pre-monsoon convective environment of pre-monsoon thunderstorms around chennai- a thermodynamical study. *Mausam, 56*(3), 659–670.

Thompson R. (2006). Explanation of SPC Severe Weather Parameters. *Storm Prediction Centre*. http://www.spc.noaa.gov/exper/mesoanalysis/help/begin.html

Tyagi, B., & Satyanarayana, A. N. V. (2010). Modeling of soil surface temperature and heat flux during pre-monsoon season at two tropical stations. *Journal of Atmosphere and Solar-Terrestrial Physics, 72*(2–3), 224–233. https://doi.org/10.1016/j.jastp.2009.11.015

Tyagi, B., Naresh Krishna, V., & Satyanarayana, A. N. V. (2011). Study of thermodynamic indices in forecasting pre-monsoon thunderstorms over Kolkata during STORM Pilot Phase 2006–2008. *Natural Hazards, 56*, 681–698. https://doi.org/10.1007/s11069-010-9582-x

Tyagi, B., & Satyanarayana, A. N. V. (2019). Assessment of difference in the atmospheric surface layer turbulence characteristics during thunderstorm and clear weather days over a tropical station. *SN Applied Sciences, 1*(8), 909. https://doi.org/10.1007/s42452-019-0949-7